


Article

Impact of Climate Forecasts on the Microbial Quality of a Drinking Water Source in Norway Using Hydrodynamic Modeling

Hadi Mohammed *, Andreas Longva and Razak Seidu 

Water and Environmental Engineering Group, Department of Ocean Operations and Civil Engineering, Norwegian University of Science and Technology (NTNU), Larsgårdsvegen 2, 6009 Ålesund, Norway; andreas.longva@ntnu.no (A.L.); rase@ntnu.no (R.S.)

* Correspondence: hadi.mohammed@ntnu.no; Tel.: +47-7016-1486

Received: 18 January 2019; Accepted: 10 March 2019; Published: 14 March 2019



Abstract: This study applies hydrodynamic and water quality modeling to evaluate the potential effects of local climate projections on the mixing conditions in Lake Brusdalsvatnet in Norway and the implications on the occurrence of *Escherichia coli* (*E. coli*) at the raw water intake point of the Ålesund water treatment plant in the future. The study is mainly based on observed and projected temperature, the number of *E. coli* in the tributaries of the lake and projected flow. The results indicate a gradual rise in the temperature of water at the intake point from the base year 2017 to year 2075. In the future, vertical circulations in spring may occur earlier while autumn circulation may start later than currently observed in the lake. The number of *E. coli* at the intake point of the lake is expected to marginally increase in future. By the year 2075, the models predict an approximately three-fold increase in average *E. coli* numbers for the spring and autumn seasons compared to current levels. The results are expected to provide the water supply system managers of Ålesund with the information necessary for long-term planning and decisions in the protection of the drinking water source. The method used here can also be applied to similar drinking water sources in Norway for developing effective risk management strategies within their catchments.

Keywords: climate change; *E. coli*; hydrodynamic modeling; lake circulation periods; precipitation; temperature

1. Introduction

The link between extreme weather events and waterborne disease outbreaks is well established in the literature [1–4]. With the imminent threat of changing climate variables on the quality of freshwater resources, water treatment plants that are heavily dependent on surface water bodies are particularly vulnerable. Microbial deterioration of surface water sources occurring during extreme precipitation events and the resulting impact on the integrity of water treatment plants and disease outbreaks have been widely investigated [5–16]. Furthermore, increasing numbers of natural organic matter in surface water sources due to changes in precipitation patterns and catchment attributes [17] may challenge the efficacy of water treatment processes, enhance regrowth of bacteria in the water distribution network, and result in waterborne disease outbreaks [18–21].

The impact of these extreme events on water supply systems is likely to be more pronounced in temperate countries, such as Norway, where seasonal variations and increases in temperature and precipitation are expected in the future. According to the Norwegian Green Paper on Climate Change Adaptation, the mean annual temperature in Norway is expected to increase from 2.3 °C to 4.6 °C by 2100, with the highest and lowest increases expected in the winter and summer months,

respectively. During the same period, annual precipitation is expected to increase from 5% to 30% with major seasonal variations and increased the frequency of torrential rains [22]. These future changes in precipitation events and temperature will lead to significant changes in water quality parameters, including the presence of microbial pathogens [23]. A study on the microbial quality of Norwegian surface water bodies showed an association between rainfall and increased loads of fecal indicator organisms into surface waters [24]. A recent study has also shown a significant association between microbial organisms in Norwegian raw water sources and changes in land use, and rainfall in the catchment [25].

Apart from rainfall, water temperature variations have been shown to affect the growth and survival dynamics of microbial organisms in raw water sources [26–29]. Variations in water temperature, which is controlled by factors such as air temperature, cloud cover, solar radiation and other geomorphometric factors [30,31], affect the hydrodynamic distribution of microorganisms through increased stratification [30–33]. In addition, the onset of heavy rains causes destratification, altering the movement of microbial organisms-bearing particles within the waterbody [34]. Short term and long-term stratification and destratification mainly resulting from temperature changes may lead to water quality deterioration [35–37]. Accordingly, the development of resilient and adaptable management strategies necessary for the provision of safe drinking water in Norway requires a quantitative estimation of the potential impact of local projections of weather parameters, such as temperature and precipitation, on the quality of raw water sources.

There is increasing reliance on models and forecasts for planning and decision-making for effective management of drinking water facilities [38–40]. Among the variety of models, properly calibrated hydrodynamic and water quality models provide reliable means of tracking primary sources of microbial contamination in drinking water sources [41–43]. In addition, these models can describe the transport of contaminants within watershed and their fate once in the waterbody [44–47]. When calibrated, hydrodynamic models can provide reliable information about the sources of microbial pathogens within catchment of a water source as well as help in identifying which source has the potential of posing the greatest threat to the microbial quality of drinking water source at the intake point. For effective planning of measures to mitigate potential health risks associated with microbial contamination of raw water sources, an assessment of potential levels of fecal indicator organisms, such as *E. coli*, in various sections of the waterbody at a particular time is imperative.

The overall aim of this study was to apply hydrodynamic modeling to assess the impact of climate change on the microbial quality of the raw water source of a water treatment plant in Norway. The specific objectives were (1) to determine the impact of discharge from the main tributaries of the lake on occurrence of *E. coli* at the raw intake point of the water treatment plant; (2) to assess the distribution of temperature in the lake and the effect on *E. coli*; (3) to evaluate how changes in climatic variables in 2045 and 2075 can affect the mixing conditions and temperature in the lake; and (4) to evaluate the effects of changes in the mixing conditions on the occurrence of *E. coli* at the raw water intake point. Developing a climate-driven microbial quality hydrodynamic model will not only provide insight into potential effects of climate change on the microbial quality of raw water, but also help managers of the water treatment plants adequately plan long-term mitigation strategies necessary for the provision of safe drinking water to the public. Further, as water treatment plants are usually designed and built with a long-life span ranging from 25 to 30 years, understanding climate impacts is critical to developing appropriate management strategies. Similar water treatment plants can, therefore, apply the method to assess the impact of climate change on their drinking water sources.

2. Materials and Methods

2.1. Study Lake and Catchment Characteristics

The hydrodynamic and water quality model was developed for the Brusdalsvatnet lake, which is located in the Møre and Romsdal Region on the west coast of Norway. The lake is the main water

source of the Ålesund water treatment plant that supplies drinking water to about 50,000 inhabitants in the city of Ålesund and adjoining communities. The drinking water treatment plant draws 28,000 m³ of water daily from the lake at a depth of 35 m at the southwestern section of the lake (Figure 1). The lake has a surface area of about 7.3 km² with a mountainous and heavily forested catchment area of approximately 30 km² and is surrounded by few settlements mostly in the northwestern and southwestern parts. In addition to the numerous smaller streams surrounding the lake, there are four major streams that drain into the lake (Figure 1). These major streams are Årsetelva, Vasstrandelva, Slettebakk and Brusdalen, with average annual flow rates of 0.15 m³/s and 0.17 m³/s, 0.08 m³/s, and 0.06 m³/s respectively. The majority of the smaller streams are either snowmelt or rainfall-induced and dry up in most parts of the year.

The lake drains into a much smaller lake called Lillevatnet, which is located at the western end of the lake. Regular rainfall in the lake catchment flushes loads of decayed organic materials from the forest catchment into the lake through the streams and overland flow. Wild animals and birds in the catchment also have the potential of contributing to the microbial contamination of the lake mainly from their droppings, and this may include *E. coli* and other pathogens of concern to human health. Within the populated areas surrounding the northwestern part of the lake, leakages from wastewater pipe network is a potential source of microbial load into the lake. Leakages and seepages from household septic tanks can also contribute to the microbial loads of the lake. Most of the houses surrounding the lake are near the shore, which makes the traveling distance of potential contamination sources short.

A previous study that analyzed water samples from streams across the lake revealed that samples collected along the northwestern end of the lake contained higher numbers of thermotolerant coliform bacteria of up to 1.95×10^4 CFU/100 mL [48]. These high numbers occurred at the populated areas within which the wastewater pipe traverses.

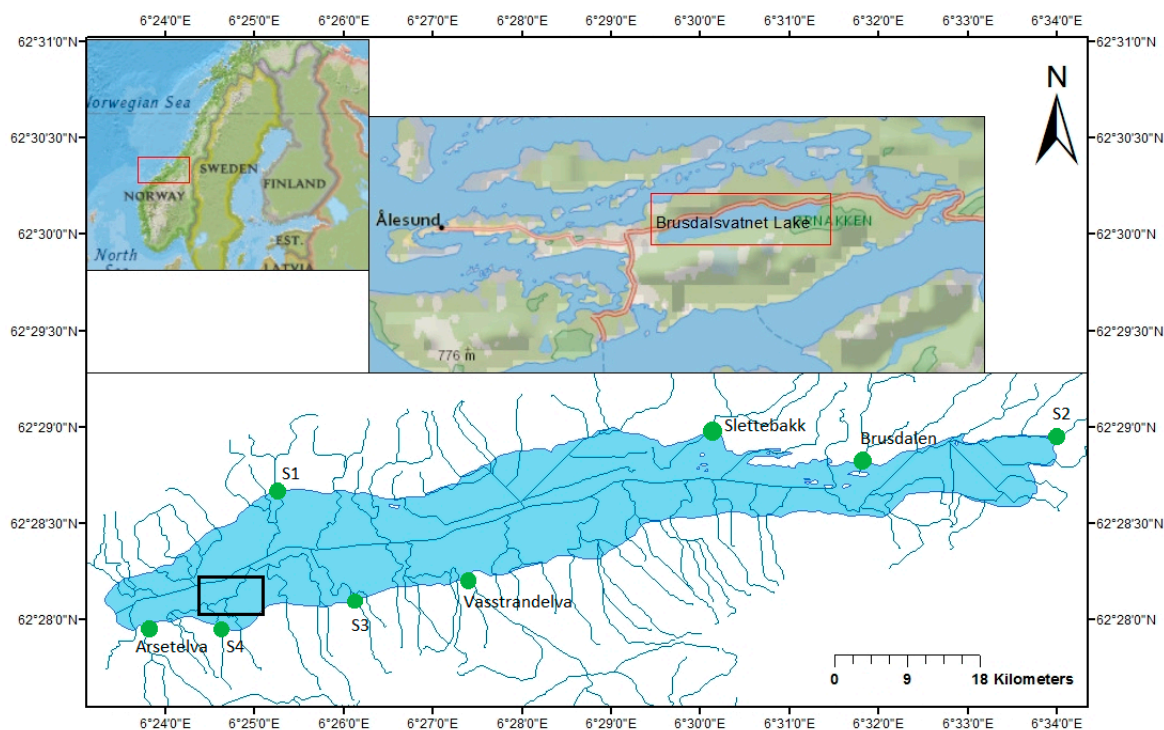


Figure 1. Map of Brusdalsvatnet Lake showing the locations of the various streams (green spots) that were sampled and the raw water intake zone of the water treatment plant (black rectangle). S1–S4 are smaller streams. The *E. coli* numbers measured in the four smaller streams were used to estimate input datasets for the unsampled areas using the area ratio method. The dark blue lines show the stream channels in the catchment of the lake.

2.2. Hydrodynamic Modeling

The data used as inputs for the hydrodynamic and water quality model included historical and projected meteorological data, hydrological data (stream flow), geographical information system (GIS) data for the shape and bathymetry of the lake, as well as historical and projected numbers of *E. coli* in the streams.

2.2.1. Hydrological Flows into the Lake

Currently, the catchment of the lake is completely ungauged. Therefore, to account for inflows and microbial discharges from various streams surrounding the lake, results of hydrological and water quality models previously calibrated for the major streams (manuscript submitted) [49] were used as inputs to the hydrodynamic model in this study. The hydrological and water quality models were based on sub-catchments using a soil and water quality modeling tool (SWAT). The SWAT is a physically based and spatially distributed hydrological model used in the simulation of water flow, sediments and contaminant transport within ungauged catchments [50,51]. Water inflows into the lake from the four major streams (Arsetelva Vasstrandelva, Slettebakk, and Brusdalen) and their sub-catchments were targeted in the hydrological modeling. The models were developed using hydrological parameter regionalization. That is, the model was initially developed for a nearby gauged lake (Engsetdalsvatnet: Lat. 62.53111, Long. 6.64889) which shares similar spatial characteristics with the target catchment (study area). These characteristics include soil type, land use, forest cover, topography, and rainfall. Daily records of precipitation and air temperature from 2010 and 2017 as well as spatial information were used in calibrating the model. The model was validated with flow measurements for Engsetdalsvatnet taken for the same period. The parameters of the model were then used in combination with precipitation, air temperature and spatial information specific to the study area to predict flow in the target streams. Further, in order to determine the catchment characteristics that mostly control runoff in the catchments (both the donor (Engsetdalsvatnet) and the target (Brusdalsvatnet)), a parameter sensitivity analysis was performed by comparing the model outputs with the measured flow at the donor catchment. In the target catchment, the flow needed for the sensitivity analysis was calculated from the donor catchment by the area ratio method. During the sensitivity analysis for both catchments, performance statistics including coefficient of determination (R^2) and Nash–Sutcliffe efficiency (NS) were calculated. Finally, the records of precipitation and air temperature were adjusted using future climate projections for the study region and used as inputs to the model for predicting potential future flows in the streams.

Hydrological model parameter regionalization as applied in this study offers an efficient means of estimating flows in ungauged catchments from gauged ones that are in proximity and share similar characteristics, such as climate, topography, soil type, and land use [52].

Once the hydrological models were developed and validated, we used the parameters in combination with historical observations of precipitation and air temperature adjusted from local climate projections for 2045 and 2075 to predict flows in the major streams for these future years. For the smaller streams (S1–S4), historical and future flows were estimated by calculating the difference between the inflows from the major streams and the sum of the outflow from the lake and withdrawal from the water treatment plant. In addition, to account for discharge from areas that were either not accessible for regular sampling (due to steep topography) or contained transient streams that only flow during high precipitation periods, we created additional discharge points during the implementation of the hydrodynamic model. Flow in the additional points was estimated from the SWAT-calibrated streams using the area ratio method. That is, after taking out the drainage areas of the streams for which the SWAT model was calibrated, the remaining catchment of the lake was divided into nine sub-catchments. The ratio of the area of each demarcated sub-catchment to the closest stream (for which SWAT model was calibrated) was calculated. Using these ratios, proportional flows in the additional discharge points were calculated from the flows calibrated for the streams in SWAT.

Table 1 shows the average historical and future flows from the SWAT model for the major streams and the calculated flows for the smaller streams. In addition, performance indices of the flow models are shown in Table 2.

Table 1. Average historical and future flows in the streams.

Stream	Flow (Historical) m ³ /s	Flow (2045) m ³ /s	Flow (2075) m ³ /s
Arsetelva	0.215	0.248	0.257
Vasstrandelva	0.273	0.246	0.252
Slettebakk	0.084	0.092	0.098
Brusdalen	0.044	0.041	0.043
S1	0.028	0.028	0.028
S2	0.021	0.021	0.021
S3	0.021	0.021	0.021
S4	0.023	0.023	0.023

Table 2. SWAT model performance indices for predicted flow in the four major streams.

Model /Stream	Nash-Sutcliff Efficiency (NS)	Coefficient of Determination (R ²)
Slettebakk	0.68	0.72
Brusdalen	0.70	0.74
Arsetelva	0.71	0.74
Vasstrandelva	0.66	0.70

2.2.2. Microbial Discharge into the Lake

Microbial discharge into the lake was accounted for by surface runoffs and direct discharges from the streams. We carried out biweekly sampling and analysis for *E. coli* in the eight streams (shown in Figure 1) between March 2017 and February 2018, and these were used as inputs to the hydrodynamic model base year (2017) scenario. The analysis of *E. coli* in the streams was performed using the membrane filtration (MF) method. In the analysis, 100 mL of the water samples were filtered through sterile, single-packed, microporous membranes with a diameter of 47 mm and pore size of $0.45 \pm 0.02 \mu\text{m}$ and with grids. After the filtration, the membranes were transferred with sterile tweezers onto coliform chromogenic agar (CCA) media (ISO 9308-1, 2000) [53] for *E. coli* cultivation at 37 °C for 24 hours. Since only eight out of the 13 discharge points were sampled for *E. coli* analysis, numbers measured in the smaller streams (S1–S4) closest to each additional discharge location were used for the remaining points.

To obtain the *E. coli* numbers required for simulating the future climate scenarios of the hydrodynamic model, *E. coli* prediction models were implemented for the four major streams as part of the flow models in SWAT. In the SWAT model, microorganisms such as *E. coli* in the catchment are introduced into hydrological response units (HRUs) in the form of dry animal manure within the catchments. In addition, mass transport and die-off/regrowth equations are used to model the discharge and die-off of *E. coli* in the soil surface layer (top 10 mm) and in the streams [54]. The SWAT was applied in predicting *E. coli* numbers in the four streams for 2045 and 2075 with adjusted catchment precipitation and air temperature for the future as inputs.

Table 3 shows a summary of the average numbers of *E. coli* in the streams for the sampling period as well as the SWAT model predictions for 2045 and 2075. The predictions from the SWAT models for 2017 were compared with the *E. coli* observed in the streams during the sampling exercise and the performance indices calculated are shown in Table 4. In terms of these indices, the *E. coli* model showed low accuracy. However, the temporal trends of the SWAT model predictions showed good agreement with the observations. The relatively low performance indices may be partly due to the sparse nature of the *E. coli* data used in evaluating the model performance. In the case of the other discharge points (including the smaller streams S1–S4), flow and *E. coli* numbers used for the baseline scenario (2017) were applied for the future scenarios (2045 and 2075) under the assumption

that two discharge points close to each other share similar spatial characteristics and potential sources of fecal indicator organisms. Since the water utility managers plan to maintain the current land use configurations within the catchment area of the raw water source over the coming years, it is assumed that the precipitation and temperature are the main factors that can significantly determine the microbial quality of the lake are rainfall and temperature. In addition, other factors, such as changes in crop types and the number of livestock and/or wild animals in the catchment, may change in the future. However, these factors were not accounted for in the modeling.

Table 3. Average numbers of *E. coli* (CFU/100 mL) in the tributaries from the monitoring exercise in 2017–2018 and the SWAT model-predicted numbers in 2045 and 2075.

Source	Average Concentration of <i>E. coli</i> (CFU/100 mL)		
	2017	2045	2075
Årsetelva	3.90×10^{-1}	1.65×10^{-1}	1.74×10^{-1}
Vasstrandelva	1.15×10^0	3.19×10^{-1}	3.36×10^{-1}
Slettebakk	2.70×10^2	2.17×10^2	2.20×10^2
Brusdalen	6.69×10^2	5.74×10^2	5.67×10^2
Stream 1	7.54×10^{-1}	7.54×10^{-1}	7.54×10^{-1}
Stream 2	3.14×10^0	3.14×10^0	3.14×10^0
Stream 3	5.89×10^{-1}	5.89×10^{-1}	5.89×10^{-1}
Stream 4	1.75×10^{-1}	1.75×10^{-1}	1.75×10^{-1}

Table 4. Performance indices of the SWAT models for *E. coli* in the four major streams.

Model /Stream	Nash-Sutcliffe Efficiency (NS)	Coefficient of Determination (R^2)
Slettebakk	0.30	0.31
Brusdalen	0.24	0.26
Årsetelva	0.32	0.31
Vasstrandelva	0.36	0.33

2.2.3. Meteorological Data

The meteorological data used in the hydrodynamic model development were obtained from the Norwegian Meteorological Institute. The weather stations included Vigra (Lat. 62.5617, Long: 6.115), Hildre (Lat. 62.6017, Long: 6.3187), and Ålesund IV (Lat. 62.4703, Long: 6.2108) and the Statens Vegvessen weather station located north of the lake. The data constituted hourly observations of air temperature, pressure, relative humidity, wind speed, and wind direction over the study area for the base year of 2017. In addition, measurements of cloud cover taken at three-hour intervals from 7 a.m. to 7 p.m. for each day were interpolated to hourly data. The model also requires hourly (or daily) temperature for the discharging streams. This was generated from the measured meteorological variables using a simple water temperature model [55] included in the Generalized Environmental Modeling System for Surfacewaters (GEMSS) model, in which the water temperature is assumed to respond only to surface heat exchange:

$$\frac{dT}{dt} = \frac{R_n}{\rho C_p} \quad (1)$$

where D is mean depth of water column, t is time, ρ is the water density, C_p is the specific heat capacity of water, and R_n , the net rate of surface heat exchange which is computed as:

$$R_n = R_s - R_{sr} + R_a - R_{ar} - R_b - R_e - R_c \quad (2)$$

where R_s and R_{sr} are transmitted and reflected shortwave solar radiation, R_a and R_{ar} are the respective longwave atmospheric radiations, R_b is back radiation, R_e is the heat loss through evaporation, and R_c is conducted heat.

For the future scenarios, the historical time series of temperature was adjusted using biase-corrected projections of air temperature in the region. The method, which is commonly used in hydrological climate impact assessments [56,57], involves transformation of historical time series of climate variables with the ratio between mean future and historical climate projections. In this study, the Norwegian Water Resources and Energy Directorate (NVE)-based temperature projections, derived from Representative Concentration Pathways (RCP 8.5) climate models for the Møre and Romsdal region of Norway, where the study site is located, were used. The RCP 8.5 projections are composed of results from ensembles of climate models (10 different models), which use the period 1971–2000 as the base year and predict climate change for up to 2100. In this model, climate projections for each year represent a 40-year average with the chosen year as the median. Therefore, the median values of the model projections for 2045 and 2075 were used in this study. The projected changes for precipitation (%) and air temperature (factor) used to adjust the historical time series for the future hydrodynamic model scenarios are shown in Table 5. Since no projections of the other weather variables (pressure, relative humidity, wind speed, wind direction, and cloud cover) were available at the time of this study, we applied the historical values to the future hydrodynamic model scenarios. Finally, GIS data for the lake shoreline and the bathymetry were used to define the boundaries of the lake for the hydrodynamic computation.

Table 5. Projected changes in climatic variables for the study region in 2045 and 2075 used in adjusting the historical time series. The values show percentage changes in precipitation and the factors (in °C) by which air temperature is expected to change.

Year	Winter	Spring	Summer	Autumn
Precipitation				
2045	0.158	14.218	9.789	−13.17
2075	−0.121	17.252	14.263	−10.78
Temperature				
2045	1.922	1.779	1.743	1.975
2075	3.374	3.241	3.112	3.409

2.2.4. Implementing the Hydrodynamic and Water Quality Models

The Generalized Environmental Modeling System for Surfacewaters (GEMSS) software [55,58] was used for the hydrodynamic and water quality models. The theoretical basis of the system computations of GEMSS is the longitudinal-vertical transport model [58] developed from the horizontal momentum balance, continuity equation, constituent transport and the equation of state. The system computes the concentration of *E. coli* in the lake as well as temperature from 3D time-varying flow fields and elevations for each computational cell of size (100 m × 100 m × 1 m) along the x, y and z dimensions of the lake.

The hydrodynamic and water quality model for the drinking water source (Brusdalsvatnet Lake) was implemented for 2017 as the baseline scenario. Finally, the flow and *E. coli* numbers predicted for the four major streams from the SWAT model (for 2045 and 2075) were applied in the same manner (as described above for creating additional discharge points for 2017). These were used to predict the hydrodynamic and water quality conditions in the lake for 2045 and 2075. The model was iteratively built using the flow and *E. coli* numbers in the streams and the meteorological data as inputs. Model calibration was performed using specifically temperature profiles measured in the lake. After each iteration of the model, outputs (mainly temperature profiles) were compared with measured temperature profiles measured in the lake. The model was initially run with higher order schemes including the Quadratic Upstream Interpolation for Convective Kinematics with Estimated Streaming Times (QUICKEST) and QUICKEST combined with Universal Limiter for Transport Interpolation Modelling of the Advective Transport Equation (QUICKEST with ULTIMATE) [59,60].

However, after repeated iterations, the outputs of these schemes showed poor fits with the measured temperature data. The best fit to the calibration data was, therefore, obtained using the upwind first order scheme. The upwind first order scheme of constituent transport was used in a fully explicit method such that all the terms that enter the computation of the constituents are derived from prevailing time steps. Computations that are based on first order upwind differencing usually suffer from false diffusion and this source of inaccuracy could be reduced by using sufficiently small grid cells. However, the use of smaller grids in this study led to model instability issues. Even though the first order scheme with the smaller grids produced instabilities, it produced the best fit in comparison with the higher order scheme. The model iterations also involved varying surface heat exchange computation parameters, such as the fraction of solar radiation reflected from the water surface, vegetation, and topographic shading factor, wind sheltering coefficient and Sechi depth, as well as ice growth model parameters including the coefficient of water-to-ice heat exchange, ice limiting temperature, and the minimum and maximum ice thicknesses. An in-depth numerical analysis of the computations that take place in each grid cell and time steps can be found in Buchack and Edinger (1984) [61]. Further, the semi-implicit transport scheme is described in Smith (2006) [62].

2.2.5. Mesh Generation

The GEMMS software used in this study is integrated with a grid generation tool. This tool was used to generate rectangular grids of dimension 100 m \times 100 m (for x and y directions) and 1 m in the vertical (z) direction. Thus, the longitudinal and lateral dimensions of the lake were divided into 100 and 25 cells respectively, with 94 vertical layers from the water surface to the bottom. Figure 2 shows the generated grids for the surface of the lake. The model was developed to simulate the temperature and *E. coli* transport in the lake for 2017. To validate the model, weekly measured water temperature profiles were compared with the outputs of the model. Subsequently, the adjusted air temperature as well as the predicted flow, and numbers of *E. coli* in the streams for 2045 and 2075 were used as inputs for simulating the future scenarios. Simulation for each year was performed from January to December with an initial lake water temperature of 4 °C, assumed from the value of 4.5 °C measured at the treatment plant in January 2017. The *E. coli* numbers for each year were entered at the same time with a first order decay rate of 0.67 per day. The output of the simulations was in the form of time series, contours and profiles put together as Access files and these were further processed to generate desired figures to be analyzed.

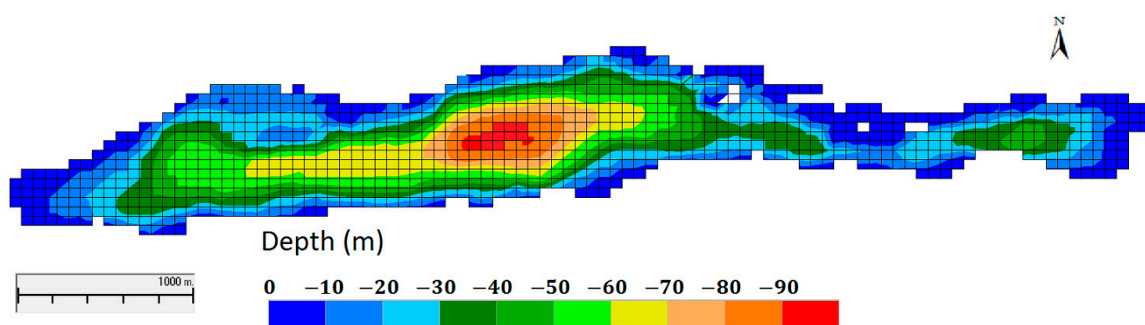


Figure 2. Computational mesh and bathymetry of Brusdalsvatnet Lake.

2.2.6. Model Validation

Validation of the model was performed graphically by plotting the temperature profiles from the model output with profiles taken in the lake by the operators of the water treatment plant. The temperature profiles were measured at six different days in the lake in 2017 at depth intervals of 5 m.

3. Results

3.1. Hydrodynamic Model Validation

Figure 3 shows a comparison of the hydrodynamic model outputs with measured temperature profiles from the water treatment plant in 2017. Although measured temperature profiles were not available for the summer months, it can be seen in the figure that the model closely predicted the profiles. Table 6 shows the performance statistics of the two transport schemes applied in calibrating the model. The values represent averages calculated from the six different profiles shown in Figure 3. As indicated in Section 2.2.4 of this study, model instabilities occurred when deficiencies associated with the first order transport scheme were resolved by applying smaller computational cells. However, the results in Table 6 indicate that despite the deficiency of this scheme, relatively higher accuracy was achieved (with the larger computational cells) in comparison with the higher order scheme (QUICKEST with ULTIMATE). Compared to the results achieved in this study, relatively higher prediction accuracies have been reported in other studies. For instance, while an R^2 value of 0.65 was obtained for the water temperature in this study, R^2 value of 0.93 was reported in the work of Bayer et al. (2013) [63], in which hydrodynamic modeling was applied in assessing the sensitivity of deep lakes to changes in climate. Similarly, root mean square errors (RMSE) ranging from 0.95 °C to 1.43 °C have been achieved in another study [64] compared with 1.22 °C achieved with the first order scheme in this study.

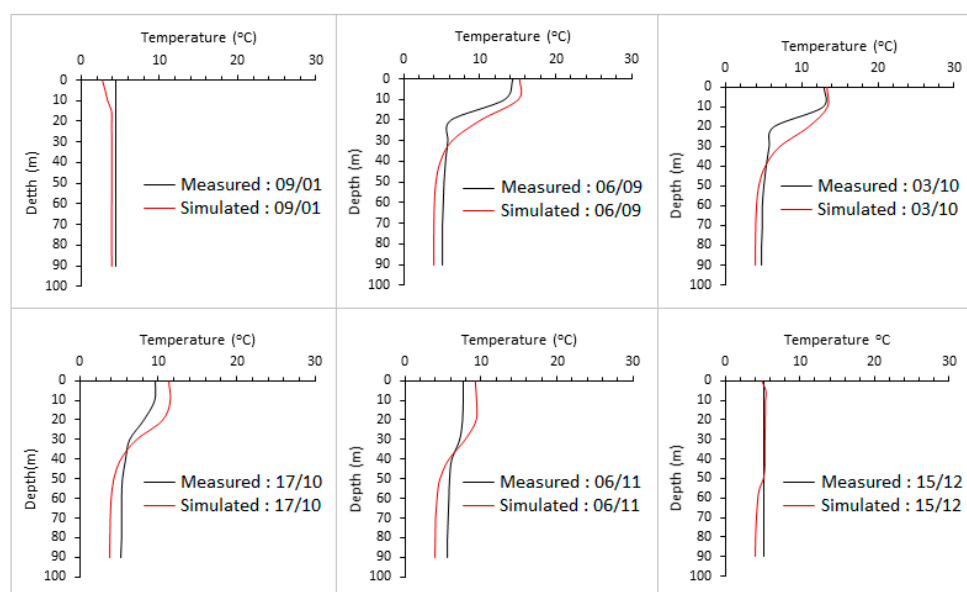


Figure 3. Measured profiles of water temperature taken in the lake on six different days in 2017. The dates on which temperature profiles were taken for model validation are shown in each sub-figure as day/month.

Table 6. Performance statistics of the transport schemes used to calibrate the hydrodynamic model against measured temperature profiles in the lake.

Transport Scheme	RMSE	R^2	Adjusted R^2
First order	1.22	0.65	0.62
QUICKEST with ULTIMATE	1.42	0.57	0.53

3.2. Simulated *E. coli* Concentration at Raw Water Intake of The Lake

As indicated in Section 2.2.4 of this study, the *E. coli* sub-module in the hydrodynamic model was not explicitly calibrated principally due to the sparse nature of the observed numbers in 2017. Vertical

temperature profiles in the lake, which was used to calibrate the model, generally give reflections of periods of vertical circulation and stratification. These processes, in turn, affect the fate and distribution of microbial organisms in the lake. Since the *E. coli* sub-module is coupled with temperature transport in the model, the accuracy of the temperature calibrations can give an indication of how well the model predicts the *E. coli* numbers in the lake. The *E. coli* numbers predicted by the model at the raw water intake depth of the lake were very low compared to the observations in 2017. In addition, both the observed *E. coli* numbers and the model outputs contained a substantial number of zero counts. Therefore, to make it possible to compare the two in a single plot (Figure 4), the numbers were expressed in CFU/L and plotted on a log scale. As shown in Figure 4, the *E. coli* numbers predicted by the model at the raw water intake depth (35 m) during the spring and autumn seasons were very low, although no observations were made by the water treatment plant managers during these seasons in 2017. The model output generally agrees with the observations in the summer season.

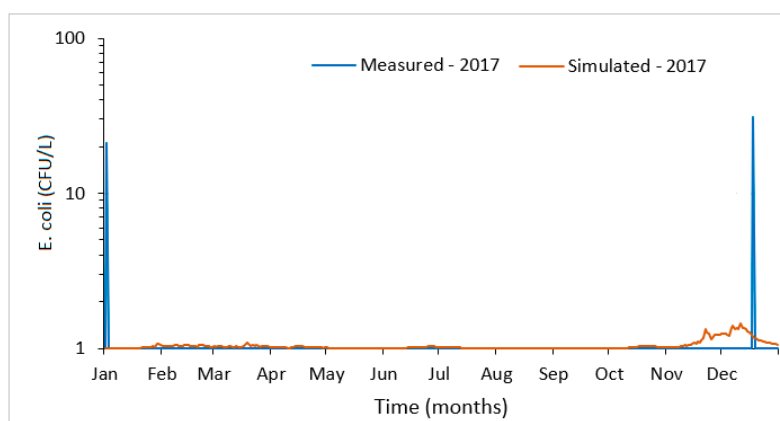


Figure 4. Simulated *E. coli* numbers at the raw water intake depth compared with observed numbers in 2017 both expressed in CFU/L and plotted on a log scale.

There were only two positive counts of *E. coli* measured at the intake point of the water utility in 2017 by the plant managers: 2 CFU/100 mL in the first week of January and 3 CFU/100 mL in the fourth week of December. Due to low flow and short periods of ice cover on the lake in winter seasons, the lake is often characterized by stratification in this season, restricting contaminant to the surface. Therefore, the occurrence of microbial pathogens at deeper sections of the lake is usually low during this period. The observations in 2017 were generally not consistent with typical trends of observations in the lake in other years. Typically, more *E. coli* observations are made in water samples from the lake during the spring and autumn seasons due to mixing (mainly from snowmelt in spring and relatively higher rainfall in autumn). This seasonal trend was predicted by the hydrodynamic model although the predictions were very low. Although the model failed to predict the observed numbers in winter, it predicted the occurrence of low numbers ($<1 \times 10^{-2}$ CFU/100 mL) in late winter (February) and in the spring months, with up to 5×10^{-2} CFU/100 mL in the autumn. This indicates that water circulation in the lake during these two seasons was predicted by the model, as this may result in the occurrence of the microorganisms at deeper parts of the lake in comparison with periods of stratification in winter and summer due to low inflows. Moreover, the low numbers from the model outputs may be an indication that the main tributaries of the lake that have been currently identified (through sampling) as major discharge points of *E. coli* into the lake may actually have a very low impact on the numbers at the raw water intake depth. Therefore, other potential non-point sources in the catchment need to be further investigated. As indicated in Section 2.1 of this study, leakages from a wastewater pipe that is close to the raw water intake section of the lake may be an important source of *E. coli* in the lake. In addition, septic tanks in some houses located in the catchment may be important contributors. Although these potential sources are located close to the shores of the lake, no specific discharge streams were identified during the sampling stage, therefore, they were not included in the

model. Further, while the model predicts the numbers without necessarily treating microorganisms as count variables, analysis of microorganisms present in water only identifies colonies that are counted. Thus, the model can predict lower numbers that are not accounted for during the analysis.

3.3. Temperature and *E. coli* Distribution in The Lake in 2017

Figure 5 shows the distribution of temperature and concentration of *E. coli* in the lake in 2017 during the four major seasons. Water circulation and vertical convective mixing mostly occurring during spring and autumn seasons characterize the lake. During the spring circulation period of 2017 (Figure 5A1), nearly isothermal conditions were observed throughout the entire depth of the lake in the western section where the raw water intake is located. In this season, the water temperature ranged from 1 °C in the top 30 m of the eastern section of the lake, to approximately 4 °C in the western part. This period of circulation can be associated with snowmelt in the catchment that leads to high flows into the lake. As shown in Figure 5A2, this circulation resulted in the dispersion of *E. coli* from the locations of high contamination sources (Slettebakk and Brusdalen streams) in the eastern section of the lake. However, the concentration of *E. coli* at the raw water intake zone in the western section was low ($<1.0 \times 10^{-4}$ CFU/100 mL).

The autumn circulation (Figure 5C1) was caused by the onset of rainfall after summer and resulted in higher temperature (~ 9 °C). While *E. coli* numbers at the 35 m depth were in excess of 5×10^{-3} CFU/100 mL, the numbers at the intake zone were relatively low ($<3 \times 10^{-3}$ CFU/100 mL) (Figure 5C2). Below this depth, the temperature was low and stratified.

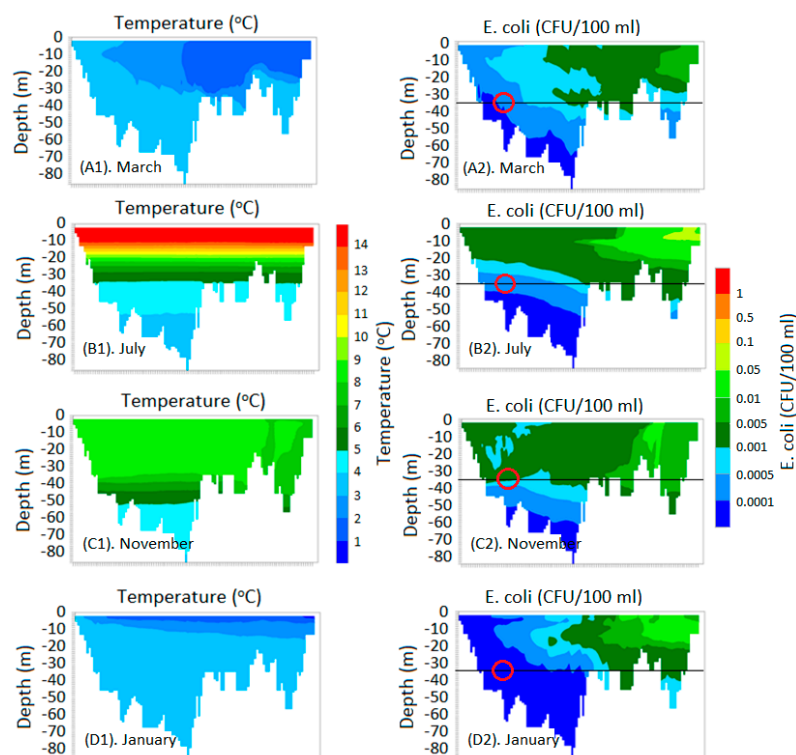


Figure 5. Cross-sections from the model output showing the distribution of temperature and *E. coli* in Brusdalsvatnet Lake in spring (A1,A2), summer (B1,B2), autumn (C1,C2), and winter (D1,D2). The black lines at 35 m depth in the lake are used to indicate the levels of *E. coli* at the raw water intake during each of the four seasons. The main withdrawal zone is shown by the red circle.

The summer condition in the lake is demonstrated by a higher temperature at the water surface reaching a maximum of approximately 17 °C in late July and early August (Figure 5B1). During this period, the deepest layers of the stratified lake remained cooler at temperatures of 4 °C. The model

also showed intense thermal stratification of the lake during this period, with a negative temperature gradient from the surface to the deeper layers. Due to the intense stratification in summer, very low concentration of *E. coli* ($< 1.0 \times 10^{-2}$ CFU/100 mL) occurs at the raw water intake zone (Figure 5B2), although the higher numbers reach deeper layers in the eastern section of the lake where the inputs from the streams were high. This can be caused by high numbers in the streams, which often occur in summer. In addition, the overall time series of the *E. coli* numbers from the observations and the model outputs were lowest in summer.

3.4. Predicted Temperature and *E. coli* in 2045 and 2075

The predicted water temperature and *E. coli* numbers in the lake are presented in Figure 6. In this figure, temperature at the surface and raw water intake depth (35 m) in the 2017 model are compared with the predictions for 2045 and 2075 (Figure 6A–C).

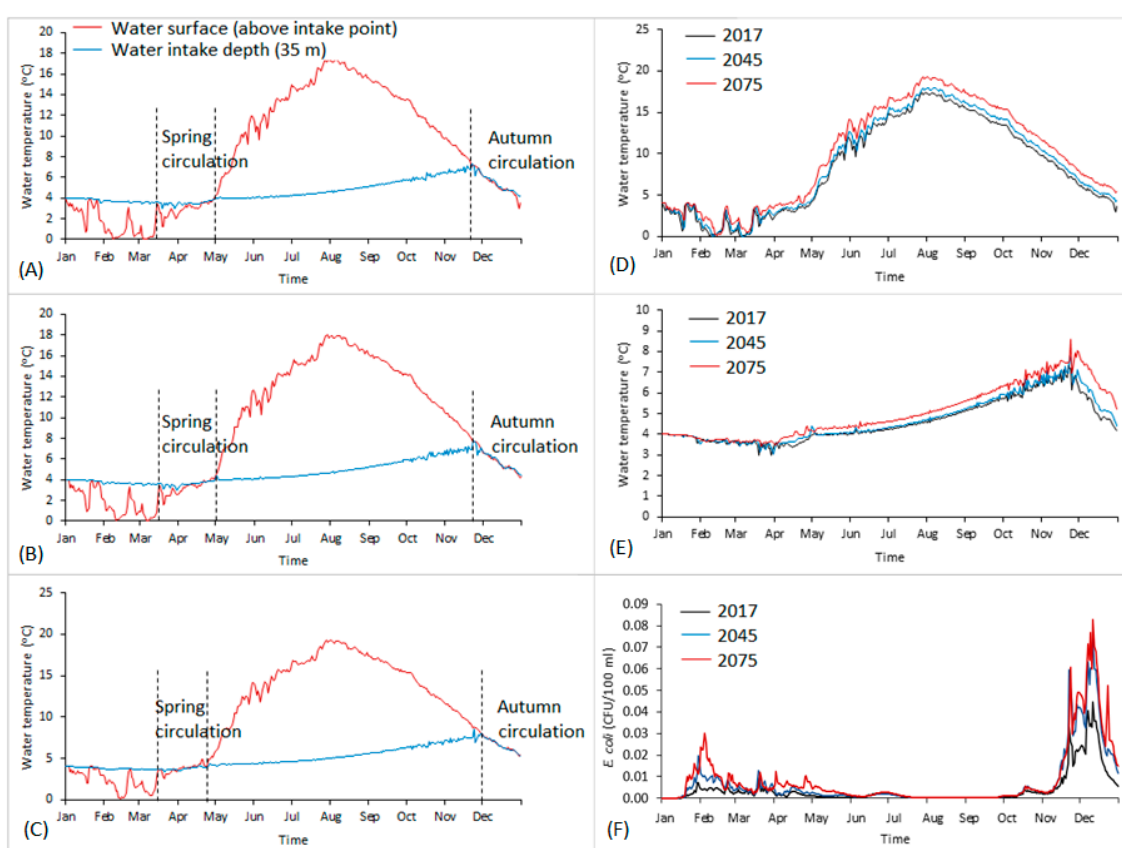


Figure 6. Comparison of temperature at the lake surface and raw water intake point for 2017 (A), 2045 (B), and 2075 (C). Increases in water surface temperature (D), intake temperature (E), and *E. coli* (F) in these years are also shown.

The model results indicate the same startup time of spring circulation for all the projected years. Similar to year 2017, spring circulation period for year 2045 starts from the middle of March and ends in late April, while the autumn circulation starts in late November. However, spring circulation in 2075 is likely to be one week shorter, ending in the third week of April. In addition, autumn circulation in this year is shifted forward by a week, starting early December. This indicates that the period of high raw water temperature may increase by 2075 due to the longer summer. Further, the intensity of spring circulation may increase in the future, as the deeper water temperature increasingly approaches that of the surface. The implication is that the chances of contaminants at the water surface reaching the deeper layers will be high due to perfect mixing. The longer summer seasons expected in the future will result in higher raw water temperature, with the surface temperature reaching 18 °C and 19 °C,

respectively, in 2045 and 2075 (Figure 6D). This will result in a higher temperature at the raw water intake depth (Figure 5E) during the autumn seasons (from 7 °C in 2017 to 8.6 °C in 2075).

The potentially late start of circulation period in the autumn seasons in future has the possibility of overriding winter conditions since the autumn circulation may extend until the start of the proceeding spring circulation. Higher numbers of *E. coli* may, therefore, occur at the intake depth of the lake throughout the autumn, winter and spring in 2045 and 2075. As shown in Figure 6F, the maximum concentration of *E. coli* at the raw water intake depth increases from approximately $<5.0 \times 10^{-3}$ CFU/100 mL in the spring of 2017 to 2.0×10^{-2} CFU/100 mL in the same season of 2075. Similarly, the concentration in autumn increases from a maximum of 4.5×10^{-2} CFU/100 mL in 2017 to approximately 9.0×10^{-2} CFU/100 mL in 2045 and 2075.

4. Discussion

The hydrodynamic model simulation showed the overall effect of the *E. coli* discharged from the streams on the *E. coli* level throughout the lake. The observed *E. coli* numbers used as input to the model resulted in a much lower level at the water intake when compared to the measured numbers at the water treatment plant. The key sources of *E. coli* load to the lake identified during the sampling were the Brusdalen and Slettebakk streams. However, the results of the model suggest that together with the four smaller streams and the additional discharge points created in the unsampled sections, discharge from the tributaries of the lake may have a low effect on the numbers of *E. coli* at the raw water intake in the lake. It is, therefore, likely that other unidentified sources of *E. coli* discharge into the lake are more dominant. For instance, households located on the western section of the lake (where the intake zone of the water treatment plant is located) could be important sources, although no overland streams were identified in this section of the catchment area during the sampling period. In addition, sewage pipes traverse this section of the lake, and there is the possibility of leakages from these pipes. It is, therefore, necessary to closely examine the pipes for potential leakages.

The model results also showed that circulation occurring in the lake in the spring and autumn increased the chances of *E. coli* reaching greater depths in the lake. Moderate rainfall at the turn over the period following the long summer season partly account for the sudden rise in the numbers of *E. coli* towards the end of November, since they favor the accumulation and transport of organic and inorganic matter into the lake through elevated stream flows. This result is consistent with a related study that reported high numbers of *E. coli* in a lake in Sweden during the same period and lowest levels in summer [65]. Further, the temperature distribution in the lake (Figure 5) indicates that considerable amount of vertical mixing of the lake water occurred during this period, thereby increasing the transport of the bacteria to the water intake point of 35 m below surface. Moreover, high-velocity wind currents, which characterize this season, enhance the circulation of water in the lake and this could increase the likelihood of contaminants reaching the intake depth.

Despite the overall very low *E. coli* numbers predicted at raw water intake zone in summer, the cross-sections indicate higher numbers potentially occurring at the same depth in the eastern section of the lake close to the dominant contamination sources identified in the sampling (Slettebakk and Brusdalen streams) as shown in Figure 5B2. The high numbers in that part may be a reflection of the high levels in the tributaries. Potential sources of *E. coli*, such as wild animals and birds in the catchment of the lake, are more active in this season and may have contributed to the observed numbers in the streams. Further, although the inactivation rates of microbial organisms in surface water generally occurs faster with increasing temperature, this dependency can be affected by site-specific conditions and can vary among different water sources [28,66]. It is, therefore, possible that typical surface water temperatures in summer in the study region create favorable conditions for the survival of *E. coli* in the streams. While high numbers of *E. coli* in the streams may be associated with catchment precipitation through increased flows and high sediment loads in spring and autumn, low flows in summer could lead to shorter travel distance and longer settling time in the streams and these may affect the numbers of microorganisms in surface water [67]. Nonetheless, the output time series

indicated generally very low numbers in the lake during the summer period (Figure 6F). This also agreed with the observation in 2017. It has been reported that other factors including lower loading of fecal materials into surface water occurring during the summer season as well as potentially less viability of fecal indicator organisms at higher water temperatures may contribute to this observed trend [68]. In addition, increased solar radiation in summer is reported as an important contributor to the inactivation of indicator bacteria in large freshwater bodies, such as lakes [69,70]. Moreover, the thermoclines in the lake during this season separate the epilimnion from the hypolimnion, restricting water circulation and the spread of contaminants in lakes [71].

The model results generally indicate the pattern of water temperature and *E. coli* in 2045 and 2075 is similar to the base year (2017). However, an increasing trend of water temperature was observed across all the seasons. Water temperature at the intake depth in spring, summer, autumn and winter rises by an average of 0.43 °C, 1.2 °C, 1.34 °C, 0.89 °C, respectively, by 2075 relative to 2017. The numbers of *E. coli* at the water intake point in future may remain at levels close to the numbers presently observed in summer. The numbers in spring and autumn may, however, be higher than present levels, with the possibility of higher numbers in winter due to the late start of the autumn circulation in the future. It is worth noting that the predicted numbers of *E. coli* at the raw water intake shown in Figure 6F only indicate the changes in the numbers relative to the present levels due to projected changes in the weather variables (air temperature and precipitation) and /stream flow. This is because the model already indicated that the discharge from the sampled streams has low effect on the occurrence of the fecal indicator bacteria at the raw water intake point (Figure 4). Thus, based on current projections of precipitation and air temperature in the study region, plans regarding the management of the drinking water facility should take into account the possibility of higher *E. coli* levels occurring in the water.

The results of this study provide useful assessments of the effect of climate change on the microbial quality of the raw water source for the treatment plant. However, the extensive use of climate data introduces considerable limitations in the use of the results, therefore management decisions that will be taken based on the results should consider such limitations. The major sources of uncertainties include the historical observations of the weather variables used in both the previous hydrological models and the hydrodynamic model, the climate projections, as well as the model formulations and their calibrations in this study. While uncertainties in the predicted stream flow and *E. coli* numbers were accounted for in the previous hydrological model [49] that provided additional inputs for this study, the number of discharge points (streams) included in the model was only a small fraction of the tributaries, most of which are either transient or cannot be easily assessed for regular sampling due to the steep topography. Thus, discharges from those sections could be higher both presently and, in the future, potentially affecting the numbers that reach the raw water intake zone. In addition, the method applied in this study only accounts for the status quo scenarios that assume all other things in the catchment of the lake will remain the same in the future. Although the water treatment plant managers plan to maintain current regulations to limit further development and recreational activities within the catchment, incidents, such as extreme precipitation events, combined sewer overflows, or bursting of sewer pipes, could potentially lead to sudden increases in the numbers of microorganisms discharged into the lake. However, such scenarios have not been accounted for in the present study.

5. Conclusions

The potential impact of climate change projections on water temperature and *E. coli* numbers in a raw water source has been examined with a focus on the Brusdalsvatnet Lake in Ålesund, Norway using a 3D hydrodynamic and water quality modeling approach. Reasonable accuracies were achieved in the water temperature predictions in the base year (2017). The results indicate that the main streams that discharge into the lake have a very low impact on the occurrence of *E. coli* at the raw water intake depth of the water treatment plant, therefore, further investigation of other important sources of contamination of the lake is required. The results for 2045 and 2075 indicate a gradual rise

in the temperature at the water intake point of the lake from the base year levels. In addition, the future models showed the likelihood of a longer autumn circulation, less protected winter season and a shorter spring circulation. Under the current climate forecasts for the catchment area of the lake, the numbers of *E. coli* in the lake, particularly at the water intake point of the treatment plant in the Ålesund water treatment plant are expected to marginally increase by 2075. The results are expected to provide the water supply managers of the water utility with the information necessary for long term planning and decisions in the protection of the water source. Moreover, with high-quality hydrological, water quality and climate data in the catchment of drinking water sources, the approach applied in this study may be useful for developing effective risk management strategies for recent and future scenarios.

Author Contributions: Conceptualization, H.M., A.L. and R.S.; Data curation, H.M.; Funding acquisition, R.S.; Methodology, H.M. and R.S.; Software, H.M. and A.L.; Writing—review & editing, H.M. and R.S.

Funding: This research was funded by the Research Council of Norway through the KLIMAFORSK project, grant number 244147/E10.

Acknowledgments: The Research Council of Norway, under the project “Impact of climate change on the association between extreme weather events and waterborne illness”, and the Ålesund water treatment plant, provided funding for this research. The authors are also grateful to the Norwegian Water Resources and Energy Directorate (NVE) and the Norwegian Meteorological Institute (MET Norway) for the provision of data. We further extend our gratitude to the Water Resource and Modeling Team of ERM Inc. for providing us with the license for the GEMSS software used in this research. Finally, we acknowledge the support and inputs provided by Bjørn Skulstad of the Ålesund Kommune.

Conflicts of Interest: The authors declare no conflict of interest.

References

1. Patz, J.A.; Hahn, M.B. Climate change and human health: A One Health approach. *Curr. Top. Microbiol. Immunol.* **2013**, *366*, 141–171. [[PubMed](#)]
2. Smith, K.R.; Woodward, A.; Campbell-Lendrum, D.; Chadee, D.D.; Honda, Y.; Liu, Q.; Sauerborn, R. Human health: Impacts, adaptation, and co-benefits. In *Climate Change 2014; IPCC: Geneva, Switzerland, 2014*; pp. 709–754.
3. Tornevi, A.; Bergstedt, O.; Forsberg, B. Precipitation Effects on Microbial Pollution in a River: Lag Structures and Seasonal Effect Modification. *PLoS ONE* **2014**, *9*, e98546. [[CrossRef](#)] [[PubMed](#)]
4. Levy, K.; Woster, A.P.; Goldstein, R.S.; Carlton, E.J. Untangling the impacts of climate change on waterborne diseases: A systematic review of relationships between diarrheal diseases and temperature, rainfall, flooding, and drought. *Environ. Sci. Technol.* **2016**, *50*, 4905–4922. [[CrossRef](#)]
5. Soh, Y.C.; Roddick, F.; Van Leeuwen, J. The future of water in Australia: The potential effects of climate change and ozone depletion on Australian water quality, quantity and treatability. *Environmentalist* **2008**, *28*, 158–165. [[CrossRef](#)]
6. Drayna, P.; McLellan, S.L.; Simpson, P.; Li, S.H.; Gorelick, M.H. Association between rainfall and pediatric emergency department visits for acute gastrointestinal illness. *Environ. Health Perspect.* **2010**, *118*, 1439–1443. [[CrossRef](#)]
7. Leppi, J.C.; DeLuca, T.H.; Harrar, S.W.; Running, S.W. Impacts of climate change on August stream discharge in the Central-Rocky Mountains. *Clim. Chang.* **2012**, *112*, 997–1014. [[CrossRef](#)]
8. Cann, K.F.; Thomas, D.R.; Salmon, R.L.; Wyn-Jones, A.P.; Kay, D. Extreme water-related weather events and waterborne disease. *Epidemiol. Infect.* **2013**, *141*, 671–686. [[CrossRef](#)]
9. Guzman Herrador, B.; De Blasio, B.F.; Carlander, A.; Ethelberg, S.; Hygen, H.O.; Kuusi, M.; Nichols, G. Association between heavy precipitation events and waterborne outbreaks in four Nordic countries, 1992–2012. *J. Water Health* **2016**, *14*, 1019–1027. [[CrossRef](#)]
10. Jagai, J.S.; Li, Q.; Wang, S.; Messier, K.P.; Wade, T.J.; Hilborn, E.D. Extreme precipitation and emergency room visits for gastrointestinal illness in areas with and without combined sewer systems: An analysis of Massachusetts data, 2003–2007. *Environ. Health Perspect.* **2015**, *123*, 873–879. [[CrossRef](#)]
11. Bezirtzoglou, C.; Dekas, K.; Charvalos, E. Climate changes, environment and infection: Facts, scenarios and growing awareness from the public health community within Europe. *Anaerobe* **2011**, *17*, 337–340. [[CrossRef](#)]

12. Bush, K.F.; O'Neill, M.S.; Li, S.; Mukherjee, B.; Hu, H.; Ghosh, S.; Balakrishnan, K. Associations between extreme precipitation and gastrointestinal-related hospital admissions in Chennai, India. *Environ. Health Perspect.* **2014**, *122*, 249–254. [[CrossRef](#)]
13. Eisenberg, M.C.; Kujbida, G.; Tuite, A.R.; Fisman, D.N.; Tien, J.H. Examining rainfall and cholera dynamics in Haiti using statistical and dynamic modeling approaches. *Epidemics* **2013**, *5*, 197–207. [[CrossRef](#)]
14. Khan, S.J.; Deere, D.; Leusch, F.D.; Humpage, A.; Jenkins, M.; Cunliffe, D. Extreme weather events: Should drinking water quality management systems adapt to changing risk profiles? *Water Res.* **2015**, *85*, 124–136. [[CrossRef](#)]
15. Barry, M.; Chiu, C.A.; Westerhoff, P. Severe Weather Effects on Water Quality in Central Arizona. *Am. Water Works Assoc.* **2016**, *108*, E221–E231. [[CrossRef](#)]
16. De Roos, A.J.; Gurian, P.L.; Robinson, L.F.; Rai, A.; Zakeri, I.; Kondo, M.C. Review of epidemiological studies of drinking-water turbidity in relation to acute gastrointestinal illness. *Environ. Health Perspect.* **2017**, *125*. [[CrossRef](#)]
17. Aryal, R.; Grinham, A.; Beecham, S. Insight into dissolved organic matter fractions in Lake Wivenhoe during and after a major flood. *Environ. Monit. Assess.* **2016**, *188*, 134. [[CrossRef](#)]
18. Hurst, A.M.; Edwards, M.J.; Chipps, M.; Jefferson, B.; Parsons, S.A. The impact of rainstorm events on coagulation and clarifier performance in potable water treatment. *Sci. Total Environ.* **2004**, *321*, 219–230. [[CrossRef](#)]
19. Bull, R.J.; Reckhow, D.A.; Li, X.-F.; Humpage, A.R.; Joll, C.; Hrudey, S.E. Potential carcinogenic hazards of non-regulated disinfection by-products: Haloquinones, halo-cyclopentene and cyclohexene derivatives, N-halamines, halonitriles, and heterocyclic amines. *Toxicology* **2011**, *286*, 1–19. [[CrossRef](#)]
20. Wang, W.; Moe, B.; Li, J.; Qian, Y.; Zheng, Q.; Li, X.F. Analytical characterization, occurrence, transformation, and removal of the emerging disinfection byproducts halobenzoquinones in water. *TrAC Trends Anal. Chem.* **2016**, *85*, 97–110. [[CrossRef](#)]
21. Abokifa, A.A.; Yang, Y.J.; Cynthia, S.L.; Pratim, B. Investigating the role of biofilms in trihalomethane formation in water distribution systems with a multicomponent model. *Water Res.* **2016**, *104*, 208–219. [[CrossRef](#)]
22. Ministry of the Environment. Adapting to a Changing Climate: Norway's Vulnerability and the Need to Adapt to the Impacts of Climate Change. Norwegian Green Paper on Climate Change Adaptation, Official Norwegian Reports NOU 2010: 10. Recommendation by a Committee Appointed by Royal Decree of 5 December 2008, Submitted to the Ministry of the Environment on 15 November 2010, Oslo. Available online: https://www.regjeringen.no/contentassets/00f70698362f4f889cbe30c75bca4a48/pdfs/nou201020100010000en_pdfs.pdf (accessed on 15 March 2017).
23. Delpla, I.; Jung, A.V.; Baures, E.; Clement, M.; Thomas, O. Impacts of climate change on surface water quality in relation to drinking water production. *Environ. Int.* **2009**, *35*, 1225–1233. [[CrossRef](#)]
24. Tryland, I.; Robertson, L.; Blankenberg, A.G.B.; Lindholm, M.; Rohrlack, T.; Liltved, H. Impact of rainfall on microbial contamination of surface water. *Int. J. Clim. Chang. Strateg. Manag.* **2011**, *3*, 361–373. [[CrossRef](#)]
25. Johannessen, G.S.; Wennberg, A.C.; Nesheim, I.; Tryland, I. Diverse land use and the impact on (irrigation) water quality and need for measures—A case study of a Norwegian river. *Int. J. Environ. Res. Public Health* **2015**, *12*, 6979–7001. [[CrossRef](#)]
26. Harvell, C.D.; Mitchell, C.E.; Ward, J.R.; Altizer, S.; Dobson, A.P.; Ostfeld, R.S.; Samuel, M.D. Climate warming and disease risks for terrestrial and marine biota. *Science* **2002**, *296*, 2158–2162. [[CrossRef](#)]
27. Vital, M.; Hammes, F.; Egli, T. Competition of *Escherichia coli* O157 with a drinking water bacterial community at low nutrient concentrations. *Water Res.* **2012**, *46*, 6279–6290. [[CrossRef](#)]
28. Pachepsky, Y.A.; Blaustein, R.A.; Whelan, G.; Shelton, D.R. Comparing temperature effects on *Escherichia coli*, *Salmonella*, and *Enterococcus* survival in surface waters. *Lett. Appl. Microbiol.* **2014**, *59*, 278–283. [[CrossRef](#)]
29. Abia, A.L.K.; Ubomba-Jaswa, E.; Momba, M.N.B. Competitive Survival of *Escherichia coli*, *Vibrio cholerae*, *Salmonella typhimurium* and *Shigella dysenteriae* in Riverbed Sediments. *Microb. Ecol.* **2016**, *72*, 881–889. [[CrossRef](#)]
30. Oswald, C.J.; Rouse, W.R. Thermal characteristics and energy balance of various-size Canadian Shield lakes in the Mackenzie River Basin. *J. Hydrometeorol.* **2004**, *5*, 129–144. [[CrossRef](#)]
31. Sharma, S.; Gray, D.K.; Read, J.S.; O'Reilly, C.M.; Schneider, P.; Quadrat, A.; Lenters, J.D. A global database of lake surface temperatures collected by in situ and satellite methods from 1985–2009. *Sci. Data* **2015**, *2*, 150008. [[CrossRef](#)]

32. Sahoo, G.; Schladow, S.; Reuter, J.; Coats, R. Effects of climate change on thermal properties of lakes and reservoirs, and possible implications. *Stoch. Environ. Res. Risk Assess.* **2011**, *25*, 445–456. [[CrossRef](#)]
33. Thorne, O.; Fenner, R. The impact of climate change on reservoir water quality and water treatment plant operations: A UK case study. *Water Environ. J.* **2011**, *25*, 74–87. [[CrossRef](#)]
34. Brookes, J.D.; Hipsey, M.R.; Burch, M.D.; Regel, R.H.; Linden, L.G.; Ferguson, C.M.; Antenucci, J.P. Relative value of surrogate indicators for detecting pathogens in lakes and reservoirs. *Environ. Sci. Technol.* **2005**, *39*, 8614–8621. [[CrossRef](#)]
35. Lawson, R.; Anderson, M.A. Stratification and mixing in Lake Elsinore, California: An assessment of axial flow pumps for improving water quality in a shallow eutrophic lake. *Water Res.* **2007**, *41*, 4457–4467. [[CrossRef](#)]
36. Shade, A.; Read, J.S.; Welkie, D.G.; Kratz, T.K.; Wu, C.H.; McMahan, K.D. Resistance, resilience and recovery: Aquatic bacterial dynamics after water column disturbance. *Environ. Microbiol.* **2011**, *13*, 2752–2767. [[CrossRef](#)]
37. Comeau, A.M.; Harding, T.; Galand, P.E.; Vincent, W.F.; Lovejoy, C. Vertical distribution of microbial communities in a perennially stratified Arctic lake with saline, anoxic bottom waters. *Sci. Rep.* **2012**, *2*, 604. [[CrossRef](#)]
38. Refsgaard, J.C.; Henriksen, H.J. Modelling guidelines—Terminology and guiding principles. *Adv. Water Resour.* **2004**, *27*, 71–82. [[CrossRef](#)]
39. Wool, T.A.; Davie, S.R.; Rodriguez, H.N. Development of Three-Dimensional Hydrodynamic and Water Quality Models to Support Total Maximum Daily Load Decision Process for the Neuse River Estuary, North Carolina. *J. Water Resour. Plan. Manag.* **2003**, *129*, 295–306. [[CrossRef](#)]
40. McIntyre, N.R.; Wheeler, H.S. A tool for risk-based management of surface water quality. *Environ. Model. Softw.* **2004**, *19*, 1131–1140. [[CrossRef](#)]
41. Hoyer, A.B.; Schladow, S.G.; Rueda, F.J. A hydrodynamics-based approach to evaluating the risk of waterborne pathogens entering drinking water intakes in a large stratified lake. *Water Res.* **2015**, *83*, 227–236. [[CrossRef](#)]
42. McCarthy, D.T.; Jovanovic, D.; Lintern, A.; Teakle, I.; Barnes, M.; Deletic, A.; Hipsey, M.R.; Bruce, L.C.; Henry, R. Source tracking using microbial community fingerprints: Method comparison with hydrodynamic modelling. *Water Res.* **2017**, *109*, 253–265. [[CrossRef](#)]
43. Zhu, X.; Wang, J.D.; Solo-Gabriele, H.M.; Fleming, L.E. A water quality modeling study of non-point sources at recreational marine beaches. *Water Res.* **2011**, *45*, 2985–2995. [[CrossRef](#)]
44. Guber, A.K.; Pachepsky, Y.A.; Yakirevich, A.M.; Shelton, D.R.; Whelan, G.; Goodrich, D.C.; Unkrich, C.L. Modeling runoff and microbial overland transport with KINEROS2/STWIR model: Accuracy and uncertainty as affected by source of infiltration parameters. *J. Hydrol.* **2014**, *519*, 644–655. [[CrossRef](#)]
45. De Brauwere, A.; Gourgue, O.; de Brye, B.; Servais, P.; Ouattara, N.K.; Deleersnijder, E. Integrated modelling of faecal contamination in a densely populated river–sea continuum (Scheldt River and Estuary). *Sci. Total Environ.* **2014**, *468*, 31–45. [[CrossRef](#)] [[PubMed](#)]
46. Liu, W.C.; Chan, W.T. Assessment of the climate change impacts on fecal coliform contamination in a tidal estuarine system. *Environ. Monit. Assess.* **2015**, *187*, 728. [[CrossRef](#)] [[PubMed](#)]
47. Sokolova, E.; Pettersson, T.J.; Bergstedt, O.; Hermansson, M. Hydrodynamic modelling of the microbial water quality in a drinking water source as input for risk reduction management. *J. Hydrol.* **2013**, *497*, 15–23. [[CrossRef](#)]
48. Berg, T. Mapping of the Inflows into Brusdalsvatnet. Ålesund Municipality Technical sector (Ålesund Kommune, Teknisk sektor), VAR-avd. 2002. Available online: <http://alesund.kommune.no/fakta-om-alesund/omkommunen/organisasjonen/item/vann-avlop-og-renovasjon> (accessed on 23 June 2016).
49. Mohammed, H.; Tveten, A.K.; Seidu, R. Modelling the impact of climate change on flow and *E. coli* concentration in the catchment of an ungauged drinking water source in Norway. **2018**, submitted.
50. Arnold, J.G.; Srinivasan, R.; Muttiah, R.S.; Williams, J.R. Large area hydrologic modeling and assessment part I: Model development. *JAWRA J. Am. Water Resour. Assoc.* **1998**, *34*, 73–89. [[CrossRef](#)]
51. Arnold, J.G.; Moriasi, D.N.; Gassman, P.W.; Abbaspour, K.C.; White, M.J.; Srinivasan, R.; Kannan, N. SWAT: Model use, calibration, and validation. *Trans. Asabe* **2012**, *55*, 1491–1508. [[CrossRef](#)]
52. Bárdossy, A. Calibration of hydrological model parameters for ungauged catchments. *Hydrol. Earth Syst. Sci. Discuss.* **2007**, *11*, 703–710. [[CrossRef](#)]

53. ISO 9308-1. *Water Quality—Enumeration of Escherichia coli and Coliform Bacteria—Part1: Membrane Filtration Method*; International Standards Organization: Geneva, Switzerland, 2000.
54. Neitsch, S.L.; Arnold, J.G.; Kiniry, J.R.; Williams, J.R. *Soil and Water Assessment Tool Theoretical Documentation Version 2009*; Texas Water Resources Institute: College Station, TX, USA, 2011.
55. ERM. *GEMSS-HDM Hydrodynamic and Transport Module, Technical Documentation*; GEMSS Development Team, Surface Water Modeling Group (SMG), ERM Inc.: London, UK, 2006. Available online: <http://www.erm-smg.com/gemss.html> (accessed on 23 April 2016).
56. Teutschbein, C.; Seibert, J. Bias correction of regional climate model simulations for hydrological climate-change impact studies: Review and evaluation of different methods. *J. Hydrol.* **2012**, *456–457*, 12–29. [[CrossRef](#)]
57. Shrestha, M.; Acharya, S.C.; Shrestha, P.K. Bias correction of climate models for hydrological modelling—are simple methods still useful? *Meteorol. Appl.* **2017**, *24*, 531–539. [[CrossRef](#)]
58. ERM. Generalized Environmental Modeling System for Surfacewaters (GEMSS). Environmental Resources Management, Inc. 2006. Available online: <http://www.erm-smg.com/gemss.html> (accessed on 23 April 2016).
59. Leonard, A. A stable and accurate convective modeling procedure based on quadratic upstream interpolation. *Comp. Methods Appl. Mech. Eng.* **1979**, *19*, 59–98. [[CrossRef](#)]
60. Leonard, B.P. The ULTIMATE conservative difference scheme applied to unsteady one dimensional advection. *Comp. Methods Appl. Mech. Eng.* **1991**, *88*, 17–74. [[CrossRef](#)]
61. Buchak, E.M.; Edinger, J.E. *Generalized Longitudinal-Vertical Hydrodynamics and Transport Development, Programming and Applications*; Prepared for U.S. Army Corps of Engineers Waterways Experiment Station, Vicksburg, Miss. Contract No. DACW39-84-M-1636. Prepared by J. E. Edinger Associates Wayne, PA. Document No. 84-18-R. June; J. E. Edinger Associates, Inc.: Wayne, PA, USA, 1984.
62. Bayer, T.K.; Burns, C.W.; Schallenberg, M. Application of a numerical model to predict impacts of climate change on water temperatures in two deep, oligotrophic lakes in New Zealand. *Hydrobiologia* **2013**, *713*, 53–71. [[CrossRef](#)]
63. Huang, A.; Rao, Y.R.; Lu, Y. Evaluation of a 3-D hydrodynamic model and atmospheric forecast forcing using observations in Lake Ontario. *J. Geophys. Res. Oceans* **2010**, *115*, C02004. [[CrossRef](#)]
64. Smith, P.E. *A Semi-Implicit, Three-Dimensional Model for Estuarine Circulation (Report No. 2006-1004)*; USGS: Sacramento, CA, USA, 2006. [[CrossRef](#)]
65. Sokolova, E.; Pettersson, S.R.; Dienus, O.; Nyström, F.; Lindgren, P.E.; Pettersson, T.J. Microbial risk assessment of drinking water based on hydrodynamic modelling of pathogen concentrations in source water. *Sci. Total Environ.* **2015**, *526*, 177–186. [[CrossRef](#)]
66. Blaustein, R.A.; Pachepsky, Y.; Hill, R.L.; Shelton, D.R.; Whelan, G. *Escherichia coli* survival in waters: Temperature dependence. *Water Res.* **2013**, *47*, 569–578. [[CrossRef](#)]
67. Schijven, J.; Bouwknegt, M.; Husman, R.; Maria, A.; Rutjes, S.; Sudre, B.; Semenza, J.C. A decision support tool to compare waterborne and foodborne infection and/or illness risks associated with climate change. *Risk Anal.* **2013**, *33*, 2154–2167. [[CrossRef](#)]
68. An, Y.J.; Kampbell, D.H.; Breidenbach, G.P. *Escherichia coli* and total coliforms in water and sediments at lake marinas. *Environ. Pollut.* **2002**, *120*, 771–778. [[CrossRef](#)]
69. Whitman, R.L.; Nevers, M.B.; Korinek, G.C.; Byappanahalli, M.N. Solar and temporal effects on *Escherichia coli* concentration at a Lake Michigan swimming beach. *Appl. Environ. Microbiol.* **2004**, *70*, 4276–4285. [[CrossRef](#)]
70. Liu, L.; Phanikumar, M.S.; Molloy, S.L.; Whitman, R.L.; Shively, D.A.; Nevers, M.B.; Rose, J.B. Modeling the transport and inactivation of *E. coli* and enterococci in the near-shore region of Lake Michigan. *Environ. Sci. Technol.* **2006**, *40*, 5022–5028. [[CrossRef](#)]
71. Boehrer, B.; Schultze, M. Stratification of lakes. *Rev. Geophys.* **2008**, *46*. [[CrossRef](#)]

